Using Near-real-time Monitoring of Landslide Deformation to Interpret Hydrological Triggers in Jiudian Gorge Reservoir

Danqing Song[1, 2], Xingbo Feng[1], Zhiqiang Wang[2] & Hongquan Song[3*]

[1]School of Naval Architecture, Ocean and Civil Engineering, Shanghai Jiaotong University, Shanghai, 200030, China

[2]School of Civil Engineering and Mechanics, Lanzhou University, Lanzhou, 730000, China

[3]Key Laboratory of Geospatial Technology for the Middle and Lower Yellow River Regions, The Ministry of Education of China, Henan University, Kaifeng, 475004, China

*[E-mail: hqsong@henu.edu.cn]

Near-real-time data with fine temporal resolution have been collected through using GPS from 105 to 130 m, and a Fast Moving Zone can be spatially identified from Main Deformation Zone, and the temporal evolution of the landslide consists of a progression in time with short periods of Fast Movement (FM) and longer periods of slower movement. The failure mode of landslide affected by rainfall is studied based on GPS monitoring data with PFC 2D being used to simulated the failure process of rain-induced landslide. Results indicate that three FMs can be identified from 105 to 130 m, and any rapid continuous drawdown of the reservoir water level from 130 to 105 m will definitely trigger FM. In addition, rapid continuous water rise tends to trigger FM from approximately 115 to 130 m while it will not trigger FMs unless there is a continuous drawdown phase before. Generally, there is a lag time between water level fluctuation and FMs.

Introduction

It is generally believed that reservoir slope instability is mainly caused by unfavorable hydrodynamic evolution in the bank due to reservoir filling[1-2]. 85% of reservoir landslides occur in the process of reservoir filling, and within two years after the first successful reservoir filling[3]. Unfavorable hydrodynamic evolution is considered the major cause leading to reservoir slope instability[4]. With the construction of the reservoir, great amounts of landslides were generated, unavoidably, along reservoir banks. Therefore, prevention of such a landslide hazard has been an urgent task in large dam projects[5], such as the Jiudian Gorge Dam Project in China.

Stability and hydrological factors contributing to landslides were continuously reported in numerous studies, and rapid water level fluctuation rainfall are two major triggers of reservoir landslides[6-11]. Model test methods[12] and detailed field investigations[13] were usually used to study the formation mechanism of landslides, with a conclusion that the water level fluctuation is the main triggering factor and rainfall is the secondary factor. The reservoir landslides were often simulated by numerical methods[14-17], such as Geostudio, FEM, PLAXIS and FLAC 3D. The data of a monitoring system obtained from inclinometers was used to interpret how the hydrodynamic condition changes and relates to landslide reactivation during

reservoir filling[2]. However, the numerical simulation method is seldom checked by systematic field instrumentation[4], and the monitoring instruments are not timely, accurate or easily operable.

Materials and Methods

In the past, the use of surface displacement data is usually considered to be the simplest way to observe the history of movement, assess the behavior of a landslide and to analyze the kinematics of movement, the response to the triggering conditions or the efficiency of corrective measures[18,19]. In addition, the basic approach is to classify movement patterns according to cumulative displacements and velocities[20-21]. Therefore, to achieve more accurate, reliable, and timely data[13], measurement of surface displacements through the use of GPS has become the most important means of tracking the behavior of landslides[14], and near real-time monitoring by using GPS has been used around the world to forecast and detect landslide activity[13,21-23]. Among these monitoring data, surface displacements from GPS have been widely used to understand the relationship between movement and hydrological triggers that mainly originate from reservoir water fluctuation, rainfall and also identify patterns of the movement[24].

It is important to monitor the hydrodynamic evolution and deformation of landslide during reservoir filling both for the investigation of reactivation mechanism and for hazard control[4]. Taking the opportunity of Jiudian Gorges Reservoir filling, a high-precision monitoring instrument (automatic GPS) is established to monitor Yanziping landslide from December 1, 2006 to December 30, 2009 in Gansu Province, China (Fig.1). It was used to identify spatial and temporal patterns of surface displacement, and to link the periods of movement to hydrological factors for detailed understanding of the hydrological triggering conditions in the period of reservoir filling. Rapid water level fluctuation is a main trigger of landslides, but the occurrence of landslide need some specific conditions before. The relationship between water fluctuation and landslide is analyzed in detail in the impoundment phase of 105~130 m (from January 1, 2009 to December 30, 2009). Moreover, the stability and failure mode of landslides affected by rainfall are also studied according to monitoring data with PFC 2D being used to verify the reliability of monitoring data.
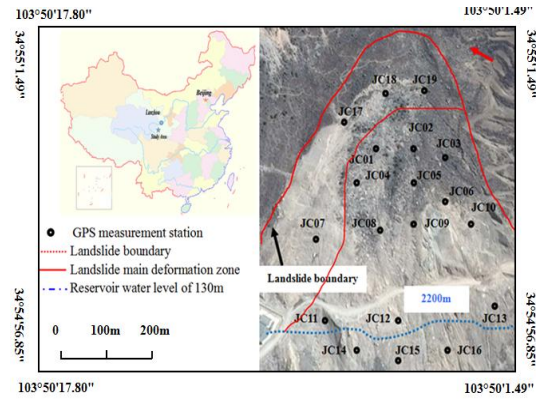
Fig.1—Location and monitoring plan of Yanziping landslide

Results and Discussion

The Yanziping landslide is a typical reservoir landslide, extending westwards from the head of Yanziping and downslope to the toe area on the bank of the Tao River, with an altitude of 2095–2360 m. Landslide is approximately 400 m wide in the north–south direction and 640 m in length in the east–west direction with the entire volume being approximately 8.94×10^6 m^3. According to detailed geological explorations and field investigations, the Yanziping landslide (Fig.2) consists of materials originating from the collapse of high and steep rock slopes and loose debris composed of talus pluvial and terrace materials. The sliding body is much looser, with a thickness of 30-73 m, and made up of limestone, gravel and loose soils. The upper layer is mainly composed of boulders, the middle layer is a mixture of stone and soil, and the lower layer is mainly composed of loose soils containing stone, gravel and sand gravel.
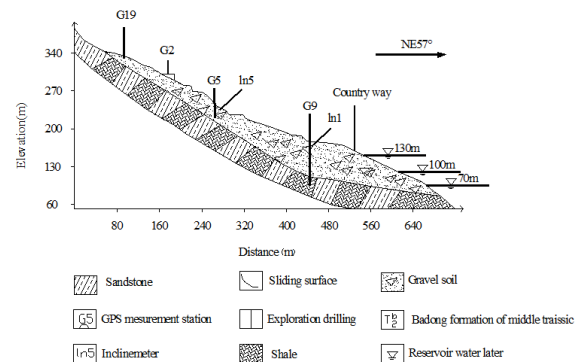
Fig.2—Schematic subsurface stratigraphy and overview photo of Yanziping landslide
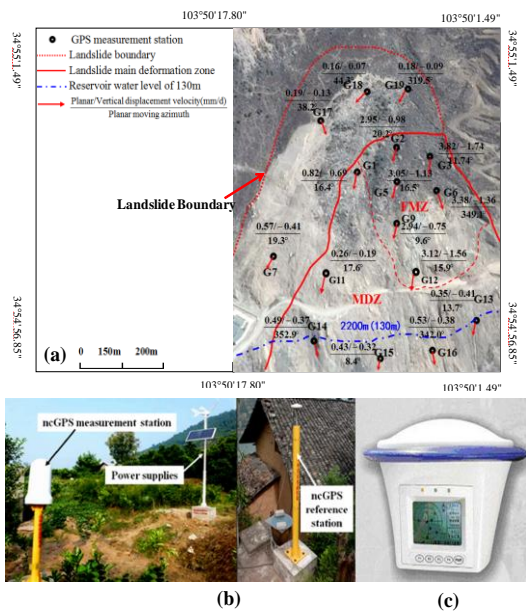
Fig.3—The monitoring network for ncGPS on the Yanziping landslide: (a) simplified geological map and monitoring network (from January 1, 2009 to December 31, 2009); (b) continuous GPS measurement station and power supplies and reference station; (c) Polaris 9600 GPS

Yanziping landslide has been monitored using the North Star 9600 GPS. Fig.3 shows the monitoring network for ncGPS on the Yanziping landslide. The measurement stations have higher measurement accuracy with 10.0 mm ± 2.0 ppm in altimetry and 5 mm ± 1.0 ppm in planimetry, and the collection frequency of the raw data can reach 5.0 Hz. Monitoring of hydrological triggering factors consists of measuring water levels of reservoir filling, water storage rate and the rainfall by analyzing the existing sources of data that can be used. These include daily reservoir water levels and rainfall that can be used from the detailed record.

Patterns of Movement

In order to study the relationship between deformation and hydrological triggering factors, the patterns of Yanziping landslide movements should be achieved an understanding firstly. Near-real-time GPS monitoring data from January 1, 2009 to December 31, 2009 are significantly valuable information, both temporally and spatially, for the interpretation of surface movement patterns.

All cumulative displacement and planar moving azimuth of GPS measurement stations from January 1, 2009 to December 30, 2009 are illustrated in Fig.3, which suggest that: (1) the obvious displacement occurred in MDZ, which has almost no deformation. For example, the planar and vertical cumulative displacement G17-G19 was only 0.25/-0.11 mm,

0.19/-0.08 mm and 0.28/-0.12mm respectively, and the moving azimuth is SW44.5°, SW36.5°, and SW41.2° respectively, which has great difference with the main slip direction; (2) within MDZ, the planar and vertical cumulative displacement are 301.3~1223.8 mm and 105.8~550.3 mm respectively, the moving azimuth is SW5.2°~SE16.7°. However, G7 control measures were taken in 2009, which resulted in it being excluded from the MDZ. Additionally, G1, which is located in the leading edge (G2) of MDZ, had minimum displacement deformation (301.3mm/-105.8mm in planimetry and altimetry), followed by G14, which is located in the western head of MDZ. Moreover, FMZ has a larger cumulative displacement that is more than 900/ 300 mm in planimetry and altimetry, including G2, G3, G5, G6, G9 and G12.

In other words, there are obvious differences in the planar azimuth, with only the deviation angle values of the planar azimuth (G17-G19) amounting to more than 30°, which suggests that significant movement only occurs in the MDZ, especially the FMZ. Therefore, only the patterns of movement in the FMZ are analyzed here. On the whole, the results suggest that there is a FMZ within the MDZ which extends from the leading edge (G2) of MDZ through the part (G1,G3,G5 and G6) to the middle area (G9).The primary slip direction is the southwest direction. On the other hand, the northwest and toe area of the MDZ have less deformation.
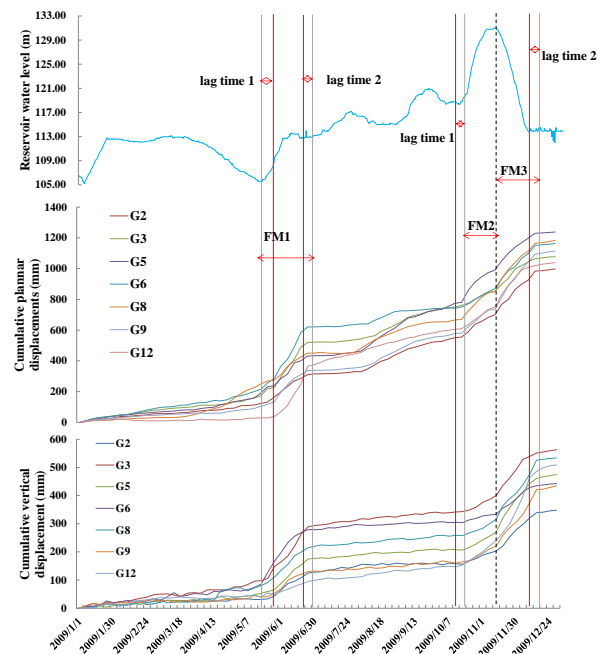
Fig.4—Time series curves of displacement of measurement stations and fluctuation of reservoir water level

The temporal evolution of the displacements of 7 GPS stations in FMZ is shown in Fig.4 In the whole year, there is a typical stepwise pattern of temporal evolution, which can be concluded from the cumulative displacements in FMZ, including two main types of motion: Short periods of faster displacement can be identified, and large magnitudes in planar/vertical displacement velocity plots were also obviously found, which lasted for a few days to weeks. In addition, longer periods of slower motion lasted most of the time. Fig.4 suggests that three FMs occurred in 2009, including FM1 (May 24–June 24), FM2 (October 18–November 13) and FM3 (November 13–December 13). The average planar and vertical moving velocity of FM1, at a speed of more than 11 mm/day and -5 mm/day respectively, was the largest, with a maximum velocity up to 13.8 mm/day in planimetry and -6.3 mm/day in altimetry. The cumulative displacement of FM3 is larger than FM2. Slower displacement occurred at slow rates that were semi-constant (about 1.25 mm/day) in both horizontal and vertical components. There are two types of lag time: lag time 1 is approximately 5 days and occurs after rapid water rise; lag time 2 appears after rapid water fluctuation (Fig.4). It is worth noting that the duration of lag time 2 is shorter than that of lag time 1.

In conclusion, there is a stepwise deformation[25] which consists of longer periods of slower motion and short periods of faster displacement in cumulative displacement plots, which means the deformation of landslide has a slow semi-constant rate, while the faster movement periods occur with a dramatic increase in moving velocity in a short period.

Triggers and Mechanism of Landslide Movements

Fig.5 shows the rate of water fluctuation and displacement velocity of the monitoring measurement stations from 105 to 130 m, by comparing the water fluctuation to the landslide movement, one notes that: (1) three faster movement correspond to certain water levels with the displacement of FMs approximately half of that in the whole monitoring period; (2) the FM1 and FM2 periods always begin with faster continuous water level rise (the rise speed is usually above 0.3 m/day); (3) FM3 occurs in the period of drawdown, and the faster displacement velocities and magnitudes have a strong positive correlation to the speed of drawdown. Therefore, the faster fluctuation of reservoir water level would trigger FMs, which means the FMs was triggered by the rapid water level fluctuation.

Obviously, Fig.5 shows that the FM1 was triggered by rapid continuous water level rise with the maximum rate of water rise reaching up to 0.4m/day, with the planar and vertical displacement at 350 and 170 mm respectively. However, the first rapid water rise that the rate of water rise was more that 0.25 m/day had little influence on the deformation of the landslide (Fig.5) with the maximum planar and vertical displacement velocities being 2.0 and 1.5 mm/day respectively. It is noticeable that a continuous drawdown occurred before the FM1, which was conducive to the much faster movement, although the deformation was small in the process of the first drawdown. In addition, the FM2 was also triggered by rapid continuous rise from 117.0 to 130.2 m with the maximum rate of water rise being approximately 0.53 m/day. However, there was no drawdown period before FM2, which is different from FM1.
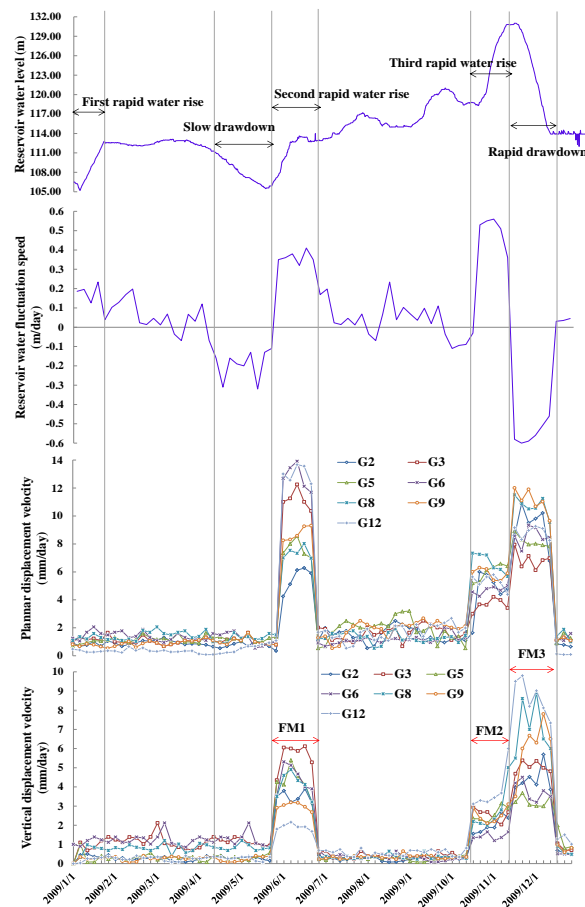
Fig.5—Time series of displacements of Yanziping landslide and reservoir water fluctuation.

In terms of FM3 that occurred after the FM2, the rate of drawdown was large at approximately 0.58 m/day with the planar and vertical velocities being 11.9 and 8.6 mm/day, which suggest that it was affected to a great extent by rapid continuous drawdown. It is worth noting that the displacement rate of FM3 was larger than that of FM2 while the deformation of the first continuous drawdown was small, which suggest the occurrence of the FM3 was closely related to the rate of drawdown and the FM2. The relationship between the FMs and the hydrological triggers is concluded as follow: FM1 and FM2 were mainly triggered by rapid continuous water level rise while FM3 was primarily triggered by the rapid reservoir drawdown with the largest speed of drawdown. In addition, the movement of the landslide shows different trends in the condition of the fluctuation of reservoir water level, a more in-depth analysis is shown in Table 1.

Table 1 shows that the movement of landslide is affected by five obvious water fluctuation periods including three main rapid water rise periods and two continuous drawdown periods. The deformation was small in the period of RWR1 due to the smaller water storage rate, approximately 0.23 m/day, which resulted in slow movement. In other words, much rapider continuous water rise means much faster movement. However, the deformation of RWR2 (FM1) was much larger than RWR3 (FM2) although the rate of water rise in FM1 was smaller due to a period of continuous drawdown (RWR1) before FM1. However, there wasn't any continuous drawdown period before FM3 compared to FM2.

Table 1—Summary of Displacements Recorded by GPS on Yanziping Landslide

Monitoring Period	Water level (m)	Rate of Water fluctuation (m/day)	Cumulative displacement (mm)		Average velocity (mm/day)		Landslide Movement
			Planar	Vertical	Planar	Vertical	
First rapid water rise (RWR1)	105.0-113.3	0.23	45.0	23.4	1.25	0.78	Slow
Second rapid water rise (RWR2)	106.1-114.0	0.35	297.5	195.6	11.2	5.1	FM1
Third rapid water rise (RWR3)	117.0-130.2	0.43	143.6	65.8	5.1	2.6	FM2
First continuous drawdown (CD1)	113.5-106.2	-0.27	150.2	74.3	1.07	0.53	Slow
Second continuous drawdown (CD2)	130.5-115.5	-0.53	213.5	189.5	8.9	7.6	FM3

In addition, three periods of rapid water rise occurred at different water levels: the first two periods appeared from 105 to 115 m, and the third one appeared from 115 to 130 m. Therefore, it can be concluded that water rise had different influences on the movement of the landslide. If the continuous drawdown of reservoir water occurs first and then the rapid continuous water rise appears in quick succession, it will for sure trigger FM from 105 to 115 m. However, the movement of the landslide will be slow without the period of continuous drawdown before a rapid water rise period. On the contrary, any rapid continuous water rise will trigger FM from 115 to 130 m with the rate of water rise being more than 0.4 m/day.

Table 1 shows the average velocity reaches 1.07 mm/day in planimetry and -0.53 mm/day in altimetry in CD1 period with the drawdown rate being -0.27 m/day, however, the average planar and vertical velocities are 8.9 mm/day and -7.6 mm/day respectively in CD2 period with the rate being 0.53 m/day. It is worth noting that the latter rate of deformation is five times as much as the former one due to the different rate of drawdown. Therefore, the drawdown of reservoir water with small rate will not trigger FMs, though the continuous drawdown lasts for a long time from 115 to 105 m, while any rapid continuous drawdown with the rates more than 0.5m /day will trigger FMs definitely from 130 to 115 m. Additionally, all of the FMs appeared in a turning period from water rise period to drawdown period, such as FM2. Moreover, if the periods of rapid water fluctuation connect in time, it will trigger much movement, such as FM3.

To quantitatively study the triggering conditions for the initiation of FMs in Yanziping Landslide, which is of significant importance in early warning of failure, a detailed analysis was used to observe the fluctuation of reservoir water levels during the three FMs periods based on ncGPS monitoring, with the results shown in Table 2. Table 2 shows that the movement of landslide was mainly triggered due to the destabilizing effects which are closely related to the rapid water rise from 105 to 130 m, and the time lag is approximately five days between continuous rapid rise and the beginning of the FMs periods, based on observations in FM1 and FM2. Moreover, the rapid continuous drawdown of reservoir water level,

with the rate being more than 0.5 m/day from 105 to 130 m, will definitely trigger FMs, as observed in the period for FM3, which indicates that much faster rates of reservoir drawdown means faster landslide movement. However, continuous drawdown with the rate less than 0.3 m/day will not trigger FMs even though it lasts for a long time, for example, the first continuous drawdown period (CD1) (Fig.4).

Therefore, the most dangerous conditions when the movement of the Yanziping landslide is triggered when: (1) rapid continuous rise of water level is from approximately 105 to 115m with a drawdown period existing before, and (2) any rapid continuous rise of water level from approximately 115 to 130 m, and (3) any rapid continuous drawdown of water level, especially the faster movement of landslide will occur after a rapid continuous water rise period. This has been observed to cause FMs of more than 4.6 mm/day in planimetry.

Table 2—Relationship between Fluctuation of Reservoir Water and Three FM Periods

Continuous rapid fluctuation of reservoir water				FM periods			Water fluctuation before
Time (2009) (start-end)	Water level (m)	Average–maximum rate	NO.	Time (2009) (start-end)	Average–maximum velocity	Lag time (start-end)	
May 24–June 24	106.1-114.0	0.35 m/day	FM 1	May 30–June 29	≥ 3.5 mm/day	5 days	Continuous drawdown
October 18–November 13	117.0-130.2	0.43 m/day	FM 2	October 23–November 18	8.7-29.5 mm/day	5 days	No Fluctuation
November 13–December 13	130.5-115.5	-0.53 m/day	FM 3	November 17–December 17	5.2–14.8 mm/day (unsure)	≤ 4 days (unsure)	Rapid water rise

According to the patterns of the movements and hydrological triggering factors, and based on extensive research on reservoir landslides[25], the deformation mechanism of the Yanziping landslide can be concluded as follows.

The slide mechanism of FM1 and FM2 is mainly affected by mechanical effects of reservoir bank slope, including dynamic water pressure effect, hydrostatic water pressure effect, and floating force effect. As water level rising, the flooding of the area increases and the effective stress of sliding surfaces and strength of sliding zone reduce, which lead to bond force and friction coefficient between particles decreasing and the sliding resistance of landslide reducing. The pore water pressure appears with underground water level rising in the landslide, and the seepage field of leading edge has great changes, which results in deformation of slope body occuring and the cracking surface expands to the deep of landslide until reaches potential shear plane. Then shear stress concentration of shear plane will occur, and the internal shear strength of rock mass is reduced. Additionally, the sliding surface is immersed by water, and virtual body pressure is greater than the actual pressure in the sliding body above the sliding surface while it produces float towing force in submerged sliding body. The effective weight sliding body immersed by water changes due to pore water pressure. Therefore, the slope stability will be reduced under the action of the former factors. However, the trigger factors between FM1 and FM2 have some differences. FM1 needs a preparation stage (continuous drawdown of water level period) in order to further much more deformation, which means the landslide was more stable from 105 to 115 m than that from 115 to 130 m. Moreover, it needs the continuous drawdown period to weaken the stability of landslide which provides a basis for the trigger of FM1.

The rapid drawdown will weaken the stability of the landslide, for example, the occurence of FM3. The speed of groundwater descent in landslide is smaller the rate of reservoir water drawdown, which leads to causing excess pore water pressure in sliding body. Besides, dynamic water pressure in landslide will increase as rapid drawdown with the landslide sliding towards the reservoir. Then the unloading effect will appear sliding body and water hammer effect also occurs in the cracks, therefore, the landslide stability will be reduced in the end.

Moreover, if there are rapid continuous water rise periods and water fall periods, it will trigger much faster movement in the later period due to the former period providing a basis for the later FM. In addition, Fig.4 shows that there are two types of lag times (Lag time 1, 2), due to an important reason that the groundwater table is changing with reservoir water fluctuation, but it lags behind the reservoir water level. Lag time 1 lasts for a longer time because the groundwater rise has a longer lag time, while lag time 2 occurs in a short period due to the fact that the groundwater level tends to be stabilized quickly.

Landslide Movements and Rainfall

Rainfall is also an important triggers of reservoir landslides in process of reservoir filling. The relationship between landslide deformation and rainfall is shown in Fig.6, which is monitored in the whole process of impoundment. Fig.6 shows that three FMs can be identified in the period of rainy season (June-September) every year. The leading edge of Yanziping landslide produced deformation failure firstly, which was affected by strong rainfall, and then the middle part of landslide pulled trailing edge, which lead to producing retrogressive landslide. Moreover, the landslide frequency is also closely related to rainfall. Fig.7 has shown positive correlation between rainfall and the landslide frequency in JGR area, for example, the frequency of landslides is largest with rainfall reaching up to the maximum in August 2008. In order to verify the reliability of GPS monitoring data, analyze the landslide failure process in depth and study the relationship critical rainfall (critical erosion velocity), particle displacement, slope and cohesive force, PFC 2D (Particle Flow Code in 2 Dimension) is used for simulating the landslide deformation process under condition of rainfall, taking two different types of slope, including noncoherent sandy soil slope and clay slope that owns larger cohesive force.
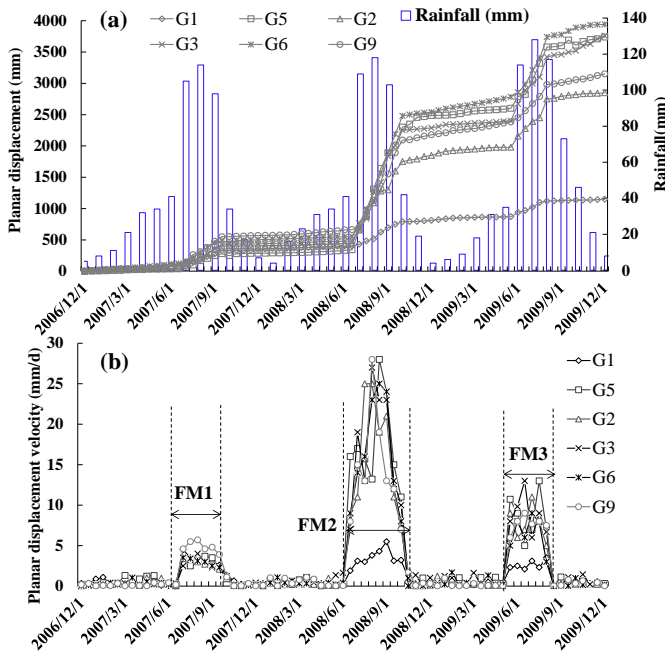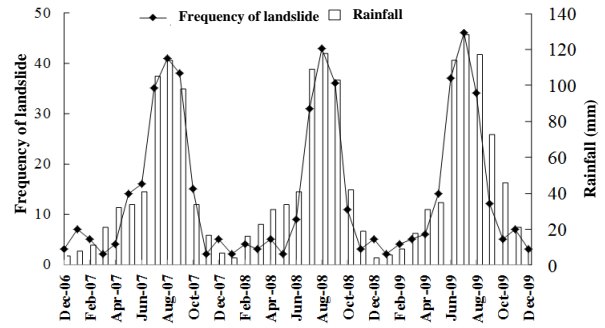
Fig.7—Time distribution of rainstorm frequency and number of landslides

The movement and interaction of circular particles can be simulated by PFC 2D (particle flow code in 2 dimensions), and the circular particles represent a individual particles of the material, such as sand, and can also on behalf of the cohesive materials. When the material is damaged gradually, the larger particles can be broken into small particles, which the cohesive materials can be divided into discrete area or block. Compared with the other discrete element programs, such as UDEC and 3DEC, PFC 2D owns a few advantages: (1) It has the potential high efficiency, because the contact detection between circular objects is simpler than that between angular objects. (2) There is no limit to simulate the displacement size in essence. (3) The larger particles can be seen as composed of small particles, and the particles can be be broken under the external load. The slope model is established based on BMP (Bonded Particle Model) model, indicating different particles are bonded together through setting cohesive force between particles of slope. To clarify the movement failure process of particles, the particles colors are divided into blue, green, light blue and red.

Taking the sandy landslide with gradient and particle size being 30° and 2 mm as an example, the failure process under condition of rainfall is shown in Fig.8a. Fig.8a shows that the particles on the surface of the slope are washed and spalled spall firstly, then the surface of the slope produces rill or shallow gully erosion, and the erode deepening gradually with the rainfall time increasing, which suggests that the slope surface produced deformation and failure firstly, and then the leading edge began to produce failure generally with the increase of rainfall time. The sliding resistance of leading edge reduced generally and lead to the slope failure from leading edge to trailing edge, however, the failure mode is the delamination failure from slope surface to depths,

Fig.6—(a) The relationship between rainfall and plannar displacements diagram; (b) The change of rate of plannar displacements diagram

which is in accordance with indoor physical model experiment results (model test 1)[26].

Taking a clay landslide with gradient and cohesive force being 30º and 80 Pa as an example, the failure mode of clay slope is shown in Fig.8b. Fig.8b shows the trailing edge of slope produced cracks firstly, and then the leading edge began to produce deformation failure as rainfall seeping into the cracks, which lead to the trailing edge producing failure finally, especially the simulation results of PFC 2D is consistent with the model test 2 (Fig.8b)[26].
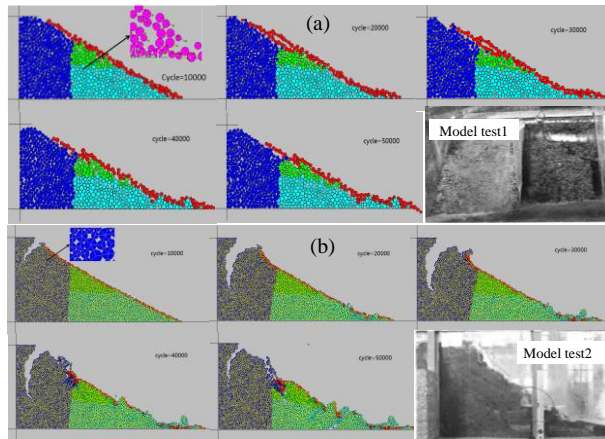
Fig.8—(a)Development process of erosion in sand slope; (b)Development process of erosion in clay slope

Due to the poor permeability of bedrock under the sliding surface, the sliding surface can be seen as the water boundary, and the landslide sliding mechanism affected by rainfall can be explained as follows. The material composition of landslide is much looser, which provides favorable conditions for rainfall infiltration. Due to the leading edge of landslide moving forward, a large number of cracks appears in the trailing edge. The rainfall infiltrates the surface cracks of landslide, and a lot of stagnant water appears in the impermeable bedrock surface, which makes sliding zone soil become saturated and also weakens the mechanical properties of sliding zone. The rainfall infiltration also makes the sliding surface soak in water, which makes the virtual body pressure is greater than the actual pressure above the sliding surface, and the lower part of the sliding body is submerged with the uplift pressure producing, therefore, the effective weight of soil soaked in water changes because of pore water pressure changing. The rainfall infiltrates the surface cracks rapidly, and the fissure water of splitting effect appears in the slide, which leads to deepening cracks and producing

through cracks. Therefore, the fast movement of landslide occurs under the condition of rainfall.

Conclusions

Based on near-real-time monitoring data of Yanziping landslide in the process of JGR filling, the moving patterns and hydraulic triggers can be defined:

At a spatial level, obvious deformation occurred in FMZ within the MDZ, which extends from the leading edge (G2) of MDZ through the part (G1, G3, G5 and G6) to the middle area (G9); in temporal terms, the movement can be defined as "Stepwise deformation" in cumulative displacement plots including longer slower motion with few short faster displacement periods. In addition, two types of lag times (Lag time 1, 2) can be found, including lag time 1 being approximately 5 days and lag time 2 being less than 4 day.

FMs were mainly triggered by rapid continuous fluctuation of water level from 105 to 130 m. For example, rapid continuous water rise was the primary triggering factor of FM1 and FM2 while FM3 tends to be triggered by rapid continuous drawdown. It is a remarkable fact that the movement will be faster if a rapid water rise period and drawdown period occur continuously, for example, in FM2 and FM3.

Rapid continuous water rise with a rate of more than 0.4 m/day tends to trigger FMs with a continuous drawdown period before FM from approximately 105 to 130 m in JGR. Any rapid continuous water rise will definitely trigger FMs from approximately 115 to 130 m. Moreover, the rapid continuous water level drawdown may well trigger FMs in process of JGR filling with the rate of drawdown reaching up to 0.5 m/day. To avoid FMs of the Yanziping landslide in the late period of reservoir filling, water rise and drawdown at slower rates (less than 0.30 m/day and less than 0.40 m/day, respectively) may be effective for the stability of the landslide. The failure mode of landslide affected by rainfall is that the leading edge produces deformation firstly and then the deformation failure of trailing edge begins to occur, which is verified by the simulation of PFC 2D.

Acknowledgments

References

1. Lin, G.W., Chen, H., Petley, D.N., et al., Impact of rainstorm-triggered landslides on high turbidity in a mountain reservoir, *Engineering Geology*, 117(1) (2011):97-103.
2. Deng, J.H., Tham, L.G., Dai, F.C., et al., Monitoring a Preexisting Landslide during Reservoir Filling, *Real Estate Economics,* 166 (2015):1-10.
3. Carvalho, R.F.D., Carmo, J.S.A.D., Landslides into reservoirs and their impacts on banks, *Environmental Fluid Mechanics*, 7(6) (2007):481-493.
4. Deng. J,, Wei, J., Min, H., et al., Response of an old landslide to reservoir filling: A case history, *Science in China Series E Engineering & Materials Science*, 48(1) (2005):27-32.
5. Petley, D.N., Landslide disaster mitigation in the Three Gorges Reservoir, China, *Mountain Research and Development*, 2010, 30(2):184-185.
6. Lee YF, Chi YY. Rainfall-induced landslide risk at Lushan, Taiwan, *Engineering Geology*, 123(1–2) (2011):113-121.
7. Chen, S.C., Chou, H.T., Chen, S.C., et al., Characteristics of rainfall-induced landslides in Miocene formations: A case study of the Shenmu watershed, Central Taiwan, *Engineering Geology*, 169(2) (2013):133-146.
8. Jiang, Q., Wei, W., Xie, N., et al., Stability analysis and treatment of a reservoir landslide under impounding conditions: a case study, *Environmental Earth Sciences*, 75(1) (2016):1-12.
9. Jiao, Y.Y., Zhang, H.Q., Tang, H.M., et al., Simulating the process of reservoir-impoundment-induced landslide using the extended DDA method, *Engineering Geology*, 182 (2014):37-48.
10. Anbalagan, R., Chakraborty, D., Kohli, A., Landslide hazard zonation (LHZ) mapping on meso-scale for systematic town planning in mountainous terrain, *J Sci Ind Res*, 67 (2008):486-497.
11. Kasiviswanathan, S.P., Subramani, T., Nesna, C., et al., Demarcation of landslide vulnerable zones in and around Achanakal, South India using remote sensing and GIS techniques, *Indian Journal of Geo-Marine Sciences*, 2009 (2014):443–446.
12. Zhou, Y.F., Tham, L.G., Yan, R.W.M., et al., The mechanism of soil failures along cracks subjected to water infiltration, *Computers and Geotechnics*, 55 (2014):330-341.
13. Huang, H., Yi, W., Lu, S., et al., Use of Monitoring Data to Interpret Active Landslide Movements and Hydrological Triggers in Three Gorges Reservoir, *Journal of Performance of Constructed Facilities*, (2015):1-10.
14. Valipour, A.A., Karami, A.A., Bidokhti., Investigating the reactions of rip current pattern and sediment transport in rip channel against changes of bed parameters using numerical simulations, *Indian Journal of Geo-Marine Sciences*, 43(5) 2014:831-840.
15. Tan, X.H., Wang, J.G., Finite element reliability analysis of slope stability, *Journal of Zhejiang University - Science A: Applied Physics & Engineering*, 10(5) (2009):645-652.
16. Sun, S.W., Chen, F.Q., Wang, W., Mechanism and Remediation of a Seismically Induced Landslide with a Potential for Deep Seated Sliding, Soil Mechanics and Foundation Engineering, 52(3) (2015):155-162.
17. Sun, S., Wang, J., Zheng, J., Analysis of a railway embankment landslide induced by the Wenchuan earthquake, China, *Soil Mechanics and Foundation Engineering*, 50(2) (2013):56-60.
18. 18 Gili, J.A., Corominas, J., RiusI, J., Using Global Positioning System techniques in landslide monitoring, *Engineering Geology*, 55(3) (2000):167-192.
19. Petley, D.N., Bulmer, M.H., Murphy, W., Patterns of movement in rotational and translational landslides, *Geology*, 30(8) (2002):719-722.
20. Massey, C.I., Petley, D.N., McSaveney, M.J., Patterns of movement in reactivated landslides, *Engineering Geology*, 159(12) (2013):1-19.
21. Allasia, P., Manconi, A., Giordan, D., et al., ADVICE: a new approach for near-real-time monitoring of surface displacements in landslide hazard scenarios, *Sensors*, 13(7) (2013):8285-8302.
22. Aleotti, P., A warning system for rainfall-induced shallow failures, *Engineering Geology*, 73(3) (2004):247-265.
23. Chen, C.Y., Chen, T.C., Yang, F.C., et al., Rainfall duration and debris-flow initiated studies for real-time monitoring, *Environmental Geology*, 47(5) (2005):715-724.
24. Du, J., Yin, K., Lacasse, S., Displacement prediction in colluvial landslides, three Gorges Reservoir, China, *Landslides*, 10(2) (2013):203-218.
25. Xu, Q., Tang, M., Xu, K.X., et al., Research on space-time evolution laws and early warning-prediction of landslides, *Chinese Journal of Rock Mechanics and Engineering*, 27(6) (2008):1104-1112.
26. Shen, S.J., Sun, H.Y., Shang, Y.Q., et al., Scouring-Penetration coupling analysis of embankment slope under rainfall action, *Chinese Journal of Rock mechanics and Engineering*, 30(12) (2011):2456-2462.